

Exotic quantum phase transitions in a Bose-Einstein condensate coupled to an optical cavity

Gang Chen,^{1,2} Xiaoguang Wang,³ J. -Q. Liang,² and Z. D. Wang^{1,*}

¹Department of Physics and Center of Theoretical and Computational Physics,
The University of Hong Kong, Pokfulam Road, Hong Kong, China

²Institute of Theoretical Physics, Shanxi University, Taiyuan 030006, China

³Zhejiang Institute of Modern Physics, Department of Physics, Zhejiang University, Hangzhou 310027, China

A new extended Dicke model, which includes atom-atom interactions and a driving classical laser field, is established for a Bose-Einstein condensate inside an ultrahigh-finesse optical cavity. A feasible experimental setup with a strong atom-field coupling is proposed, where most parameters are easily controllable and thus the predicted second-order superradiant-normal phase transition may be detected by measuring the ground-state atomic population. More intriguingly, two novel quantum phase transitions, one is a *first-order* normal phase to “Mott” phase and the other corresponds a *second-order* superradiant phase to “Mott” phase, are also revealed. In addition, a rich and exotic phase diagram is presented.

PACS numbers: 03.75.Kk, 42.50.Pq

As is known, a trapped Bose-Einstein condensate (BEC) may be used to generate a macroscopic quantum object consisting of many atoms that are in the same quantum state with a longer lifetime and can be excited by either deforming the trap or varying the interactions among atoms. Thus the BEC, as a distinct macroscopic quantum system, plays an important role in the in-depth exploration of both fundamental physics and quantum device applications of many-body systems [1]. In particular, an intriguing idea to combine the cavity quantum electrodynamics (QED) with the BEC has recently attracted significant interests both theoretically and experimentally as many exotic quantum phenomena closely related to both light and matter at ultimate quantum levels may emerge [2, 3, 4, 5, 6, 7, 8, 9, 10, 11, 12, 13].

Very recently, a so-called strong coupling of a BEC to the quantized field of an ultrahigh-finesse optical cavity was realized experimentally [14], which not only implies that a new challenging regime of cavity QED has been reached, where all atoms occupying a single mode of a matter-wave field that can couple identically to the photon induced by the cavity mode, but also opens a wider door to explore a variety of new quantum phenomena associated with the cavity-mediated many-body physics of quantum gas. Regrettably, the authors of Ref. [14] ignored the important nonlinear interactions among the untracold atoms that are controllable via the Feshbach resonance technique, while these interactions are believed to have also a considerable impact on physical properties of the BEC, leading to some exotic quantum phenomena [15].

In this Letter, we establish an extended Dicke model with the atom-atom interactions and a driving classical laser field under the two-mode approximation. A feasible experimental setup with the remarkable controllable parameters including a collective strong atom-field coupling is proposed. We illustrate how to drive a well-known second-order superradiant-normal phase transition and how to detect it experimentally. Remarkably, this superradiant phase transition was predicted in quantum optics many years ago, but has never been observed in experiments [16, 17, 18, 19, 20, 21, 22]. More intriguingly, the novel *first-order* normal to “Mott” and *second-*

order superradiant to “Mott” phase transitions are also revealed. In addition, we also obtain a rich and exotic phase diagram covering phenomena from quantum optics to the BEC, which is attributed to the competition between the atom-atom and the atom-field interactions.

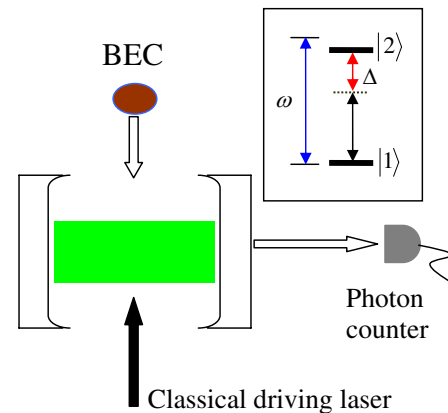


FIG. 1: (Color online) Schematic diagram of an experimental setup for a BEC of ^{87}Rb atoms coupled to a QED cavity. The BEC with two levels $|1\rangle$ and $|2\rangle$ is prepared in a time-averaged, orbiting potential magnetic trap. After moving the BEC into an ultrahigh-finesse optical cavity, an external controllable classical laser is applied to produce various transitions of the atoms between $|1\rangle$ and $|2\rangle$ states.

Our proposed experimental setup is depicted in Fig. 1. For an optical cavity with length $176\ \mu\text{m}$ and the mode waist radius $27\ \mu\text{m}$, we may choose the parameters of the cavity $(g_0, \kappa, \gamma) = 2\pi \times (10.6, 1.3, 3)\ \text{MHz}$ [14], where g_0 is the maximum single atom-field coupling strength, κ and γ are the amplitude decay rates of the excited state and the intracavity field, respectively. Such a choice implies that the system is in the strong coupling regime, and thus the long-range coherence could be well established and the quantum dissipation effect may be safely neglected. Based on a pair of coupled Gross-Pitaevskii equations for the BEC with two lev-

els $|F = 1, m_f = -1\rangle$ ($|1\rangle$) of $5^2S_{1/2}$ and $|F = 2, m_f = 1\rangle$ ($|2\rangle$) of $5^2P_{3/2}$ and under the two-mode approximation, the total Hamiltonian for the elastic two-body collisions with the interaction potential of δ -functional type may be written as

$$\hat{H} = H_{ph} + H_{at} + H_{at-at} + H_{at-cl} + H_{at-ph} \quad (1)$$

with $H_{ph} = \omega a^\dagger a$ ($\hbar = 1$ hereafter), $H_{at} = \omega_1 c_1^\dagger c_1 + (\omega_2 + \omega_{12}) c_2^\dagger c_2$, $H_{at-at} = \eta_1 c_1^\dagger c_1^\dagger c_1 c_1 / 2 + \eta_2 c_2^\dagger c_2^\dagger c_2 c_2 / 2 + \chi c_1^\dagger c_1 c_2^\dagger c_2$, $H_{at-cl} = \Omega [c_1^\dagger c_1 \exp(-i\varpi t) + c_1^\dagger c_2 \exp(i\varpi t)] / 2$, and $H_{at-ph} = \tilde{\lambda} (c_1^\dagger c_2 + c_2^\dagger c_1) (a^\dagger + a)$, where a is the annihilation operator of the cavity mode with frequency ω ; c_1 and c_2 are the annihilation boson operators for $|1\rangle$ and $|2\rangle$, respectively; $\omega_l = \int d^3\mathbf{r} \{ \phi_l^*(\mathbf{r}) [-\nabla^2 / 2m_R + V(\mathbf{r})] \phi_l(\mathbf{r}) \}$ ($l = 1, 2$) with $V(\mathbf{r})$ being a single magnetic trapped potential of frequencies ω_i ($i = x, y, z$) and m_R being the atomic mass; ω_{12} is the atomic resonance frequency; $\eta_l = (4\pi\rho_l/m_R) \int d^3\mathbf{r} |\phi_l(\mathbf{r})|^4$ and $\chi = (4\pi\rho_{1,2}/m_R) \int d^3\mathbf{r} |\phi_1(\mathbf{r})|^2 |\phi_2(\mathbf{r})|^2$ with ρ_l and $\rho_{1,2}$ ($= \rho_{2,1}$) being the intraspecies and the interspecies s -wave scattering lengths, respectively; $\Omega = 2\Omega_0 \int d^3\mathbf{r} \phi_2^*(\mathbf{r}) \phi_1(\mathbf{r})$ with Ω_0 being the Rabi frequency for the introduced classical laser with a driving frequency ϖ ; and $\tilde{\lambda} = \tilde{g} \int d^3\mathbf{r} \phi_1^*(\mathbf{r}) \phi_2(\mathbf{r}) = \tilde{g} \int d^3\mathbf{r} \phi_1^*(\mathbf{r}) \phi_2(\mathbf{r})$ with \tilde{g} being a interaction constant between the atom and the photon [23].

Under a unitary transformation $U = \exp(-i\varpi J_z t)$ and using the Schwinger relations: $J_x = (c_2^\dagger c_1 + c_1^\dagger c_2) / 2$, $J_y = (c_1^\dagger c_2 - c_2^\dagger c_1) / 2i$, and $J_z = (c_1^\dagger c_1 - c_2^\dagger c_2) / 2$ with the Casimir invariant $J^2 = N(N/2 + 1) / 2$, Hamiltonian (1) can effectively be rewritten as

$$H = \omega a^\dagger a + \frac{\lambda}{\sqrt{N}} J_x (a^\dagger + a) + \omega_0 J_z + \Omega J_x + \frac{v}{N} J_z^2, \quad (2)$$

where $\lambda = 2\tilde{\lambda}\sqrt{N}$ denotes a collective coupling strength, $v = N[(\eta_1 + \eta_2)/2 - \chi]$ describes the atom-atom interactions including the repulsive ($v > 0$) and attractive ($v < 0$) interactions, and $\omega_0 = \omega_2 - \omega_1 + (N-1)(\eta_2 - \eta_1)/2 + \Delta$ with $\Delta = \omega_{12} - \varpi$ being the detuning. For a single trapped potential, we have $\omega_2 = \omega_1$ and consider only the case of $\rho_1 = \rho_2$, which has the advantages that it reduces the effects of fluctuations in the total atomic number and ensures a large spatial overlap of different components of the condensate wavefunction. Thus, the parameters v and ω_0 can further be reduced to $v = N(\eta_1 - \chi)$ and $\omega_0 = \Delta$. Eq. (2) is a key result, which describes the collective dynamics for the composite system and has a rich phase diagram. Here we refer this equation to as an *extended Dicke model* since it contains the extra laser field term (the 4-th one) and atom-atom interaction term (the 5-th one) in comparison with the standard Dicke model and its generalized version [16, 17, 18, 19, 20, 21, 22].

A distinct property of Hamiltonian (2) lies in that all parameters can be controlled independently. For example, the effective coupling strength λ can be manipulated by a standard technique. The effective Rabi frequency Ω and the detuning Δ depend on the experimentally controllable classical

laser, and especially, the detuning Δ can vary continuously from the red ($\Delta < 0$) to the blue ($\Delta > 0$) detunings. The parameters v ranging from the positive to the negative is determined by the s -wave scattering lengths via Feshbach resonance technique [15]. For $v = 0$ ($\rho_{1,2} = \rho_1$) and $\Omega = \varpi = 0$, Hamiltonian (2) is reduced to a standard Dicke model with a second-order superradiant phase transition at the critical point $\lambda_c = \sqrt{\omega\omega_0}$ [16, 17, 18, 19, 20, 21, 22]. It should be noticed that this important prediction has never been observed in experiments. The main difficulties are likely (i) all atoms can hardly interact identically with the same quantum field; (ii) the frequencies ω and ω_0 typically exceed the coupling strength λ by many orders of magnitude; (iii) it is hard to control the parameters as demanded. However, in our proposal, these difficulties could be completely overcome by using the currently available experimental techniques of BEC, as will readily be seen below.

To explore quantum phases and their transitions, we now investigate the ground-state properties of Hamiltonian (2), which can approximately be dealt with by using the Holstein-Primakoff transformation, $J_+ = b^\dagger \sqrt{N - b^\dagger b}$, $J_- = \sqrt{N - b^\dagger b} b$ and $J_z = (b^\dagger b - N/2)$ with $[b, b^\dagger] = 1$. Here we introduce two shifting boson operators $c^\dagger = a^\dagger + \sqrt{N}\alpha$ and $d^\dagger = b^\dagger - \sqrt{N}\beta$ with auxiliary parameters α and β to describe the collective behaviors of both the atoms and the photon [19, 20, 21, 22]. With the help of the boson expansion method, the scaled classical energy can be given by $E_0(\alpha, \beta)/N = \omega\alpha^2 - 2\lambda\alpha(h^2 - 1/2) + \Delta h\sqrt{1 - h^2} + \Omega(h^2 - 1/2) + v h^2(1 - h^2)$ with $\beta^2 = h\sqrt{1 - h^2} + 1/2$. When $\alpha = \lambda(h^2 - 1/2)/\omega$ and the equilibrium condition $\partial[E_0(h)/N]/\partial h = 0$ is considered, an equation can be obtained by

$$2(u + v)\eta(1 - \eta^2) + 2\Omega\eta(1 + \eta^2) + \Delta(1 - \eta^4) = 0, \quad (3)$$

where $h = \eta/\sqrt{1 + \eta^2}$ and $u = \lambda^2/\omega$. The coefficient ($u + v$) describes the intrinsic competition between the atom-atom and the atom-field interactions and gives rise to some exotic phase transitions predicted in the following.

Equation (3) contains the basic information of quantum phases and their transitions. As a benchmark, we first address the simplest case that there is no nonlinear interaction among atoms, namely, $v = 0$ ($\rho_1 = \rho_{1,2}$). Fig. 2 shows the scaled ground-state energy $E_0/N = -u[(1 - \eta^2)/2(1 + \eta^2)]^2 + \Delta\eta/(1 + \eta^2)$ and atomic population (or equivalently ‘‘magnetization’’) $m/N = 2\langle J_z \rangle / N = 2\eta/(1 + \eta^2)$ as a function of the detuning Δ for different Rabi frequencies (Ω). It can be seen clearly that in the limit $\Omega \rightarrow 0$, this system exhibits collective excitations of both the atom and the field with macroscopic occupations (i.e., $|m/N| < 1$ and $\langle a^\dagger a \rangle > 0$) for $-u < \Delta < u$, whereas there are no such excitations for $\Delta > u$ and $\Delta < -u$ (the solid black line). This interesting behavior typically shows the second-order superradiant phase transition in quantum optics with the critical point $\Delta_c = \pm u$ [16, 17, 18, 19, 20, 21, 22]. Moreover, here we can easily achieve the condition that the order of magnitude of λ is the

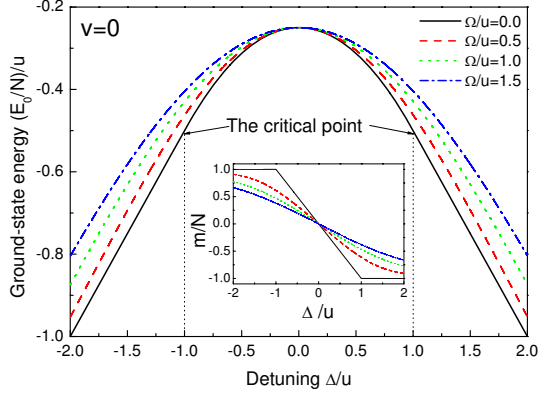


FIG. 2: (Color online) The scaled ground-state energy E_0/N and atomic population m/N (Insert part) versus the detuning Δ for different Rabi frequencies (Ω) at $v = 0$.

same as that of $\sqrt{\omega\Delta}$ by controlling the detuning of the classical laser, which means that our proposed composite system with the controllable classical laser is a promising candidate for exploring cavity-induced superradiant phase transition by measuring the ground-state atomic population via the resonant absorption imaging [24]. When the Rabi frequency Ω is increased, this second-order superradiant phase transition disappears.

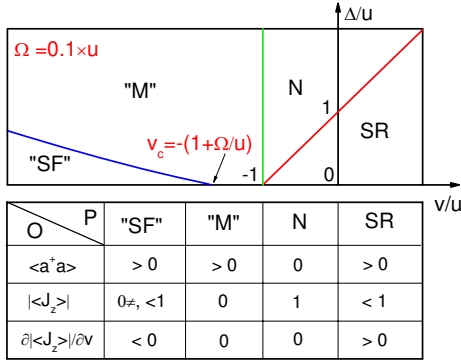


FIG. 3: (Color online) A zero-temperature phase diagram of the detuning Δ and the atom-atom interaction strength v with a low Rabi frequency Ω . The blue line is a schematic curve and is actually determined by $\Delta = \pm[(u+v)^{2/3} - \Omega^{2/3}]^{3/2}$. Two second-order phase transitions occur when crossing the red and blue lines, and a first-order phase transition happens at the green line except for $v = -u$. Note that this phase diagram is symmetric with respect to $\Delta < 0$, simply because the Hamiltonian (2) is invariant under the transformation $\Delta = -\Delta$ and $J_z = -J_z$. The lower Table denote four different quantum phases. Here, "SF"="Superfluid" phase, "M"="Mott" phase, N=Normal phase, SR=Superradiant phase, P=phase, and O=order parameter.

In fact, the nonlinear interactions among atoms controlled by Feshbach resonance technique play an important role for

the ground-state properties. Fig.3 plots a zero-temperature phase diagram for the atom-atom interaction strength v and the detuning Δ with a low Rabi frequency in the framework of mean field. The Table lists the corresponding ranges of the mean intracavity photon number $\langle a^\dagger a \rangle$, the atomic population $\langle J_z \rangle$, and the "susceptibility" $\partial \langle J_z \rangle / \partial v$ for four different quantum phases. In the case of the repulsive interaction ($v > 0$), the critical point becomes $\Delta_c = \pm(u+v)$, which implies that an effective atom-field interaction is enhanced, while in the weak attractive interaction case ($-u < v < 0$), the effective interaction is suppressed. However, the basic features of the superradiant phase transition remain. In particular, in the case of $v = -u$, this system exhibits two novel phase transitions. One is a *first-order* normal to "Mott" phase transition except for $\Delta = 0$ (Green line). The other is a *second-order* phase transition from the superradiant to the "Mott" phases at $\Delta = 0$ [25]. The relevant physics can be intuitively understood as following. In an optical cavity with $\omega \gg \lambda$, the cavity mode is only weakly or virtually excited, and the energy term $\omega a^\dagger a + (\lambda/\sqrt{N})J_x(a^\dagger + a)$ is therefore nearly equal to $-vJ_x^2/N$. If $v > -u$, the ground-state properties in the low Rabi frequency regime are governed by the energy $-|u+v|J_x^2/N + \Delta J_z$. In the vicinity of $\Delta = 0$, the effective potential in the Landau-Ginzburg theory is a double-well potential with the photon-assisted Josephson tunneling, which means that this system is located at the superradiant phase. If $-u - \Omega < v < -u$, the energy $-|u+v|J_x^2/N + \Delta J_z + \Omega J_x$ is dominant and the corresponding effective potential is a single-well potential with no internal Josephson tunneling, leading to the same atomic numbers for the two levels ($m = 0$), which may be referred to as the "Mott" phase [26]. Also, when v is decreased, a second-order phase transition from the "Mott" to the "superfluid" phases (Blue line) occurs at the critical point $v_c = -u - [\Omega^{2/3} + \Delta^{2/3}]^{3/2}$. In the so-called "superfluid" case, the effective potential is another double-well potential with the internal Josephson tunneling induced by the attractive interaction [26]. It should be pointed out that these four different phases can be distinguished experimentally by measuring the atomic population $\langle J_z \rangle$ and the "susceptibility" $\partial \langle J_z \rangle / \partial v$. In the limit $\Omega \rightarrow 0$, this predicted second-order phase transition from the superradiant to the "Mott" phases becomes a direct transition from the superradiant to the "superfluid" phases with the same order at the critical point $v_c = -u$ and $\Delta = 0$.

Although the second-order superradiant phase transition disappears in the strong attractive interaction ($v < -u$), another interesting phase transition (from the phase with nonzero macroscopic occupation of the level 1 to that of the level 2) in the "superfluid" regime emerges when the detuning Δ changes from negative to positive (i.e., from the red to the blue detunings). Fig. 4 shows the scaled atomic population m/N versus Δ for different Ω s. We see that a novel *first-order* "superfluid" phase transition occurs at $\Delta = 0$, and moreover this first-order phase transition exists until $\Omega_c = |u+v|$ (Red dashed line). For $\Omega = \Omega_c$, it becomes a *second-order* phase transition with the same critical point. For $\Omega > \Omega_c$, no phase

transition has been seen by varying Δ .

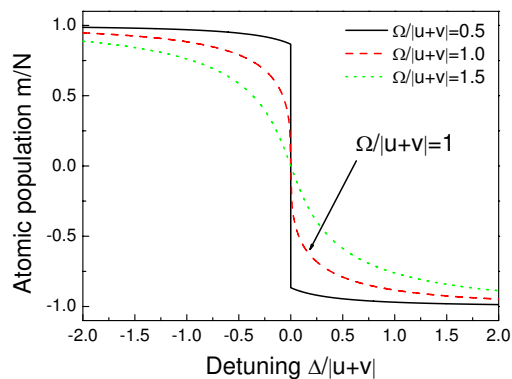


FIG. 4: (Color online) The scaled ground-state atomic population m/N versus the detuning Δ for different Rabi frequencies Ω when $v < -u$.

We now estimate the energy scales for the parameters in Hamiltonian (2) to address the experimental feasibility. Under the two-mode approximation, the wavefunctions of the macroscopic condensate states for the single magnetic trap may roughly be approximated by $\phi_l(\mathbf{r}) = \pi^{-3/4} (d_x d_y d_z)^{-1/2} \exp[-(x^2/d_x^2 + y^2/d_y^2 + z^2/d_z^2)/2]$ with $d_x = \sqrt{1/m_R \omega_x}$, $d_y = \sqrt{1/m_R \omega_y}$ and $d_z = \sqrt{1/m_R \omega_z}$. Hence, the atom-atom interaction strength can be estimated by $v = N(\rho_1 - \rho_{1,2})/\sqrt{2\pi} d_x d_y d_z m_R$. For the typical values $(\omega_x, \omega_y, \omega_z) = 2\pi \times (290, 43, 277)$ Hz, $\rho_1 = 4.2$ nm, $\rho_{1,2} = 9.7$ nm, and $m_R = 1.45 \times 10^{-25}$ kg, the energy scale of v is about -0.238 MHz with $N = 5 \times 10^4$, which ensures that the error (the order of $1/\sqrt{N}$) for determining the ground-state properties by means of the Holstein-Primakoff transformation is very low. The effective coupling strength $\lambda = 2\tilde{\lambda}\sqrt{N} = 2.81 \times 10^4$ MHz for $\tilde{\lambda} = 2\pi \times 10$ MHz [14] is indeed in the strong coupling regime. The energy scale for u is about 0.315 MHz for $\omega = 2.51 \times 10^9$ MHz [14], which can be adjusted by controlling the frequency of photon. These energy scales for u and v imply that the intrinsic competition between the atom-atom and atom-field interaction should be taken into account seriously in the BEC coupled to the optical cavity.

Finally, we elaborate briefly how to probe the predicted phase transitions experimentally. From the condition $\alpha = \lambda(\eta^2 - 1)/2\omega(\eta^2 + 1)$ with $\lambda = 2.81 \times 10^4$ MHz and $\omega = 2.51 \times 10^9$ MHz, we can immediately evaluate the maximum of the scaled mean intracavity photon number $\langle a^\dagger a \rangle / N$ and find it to be much less than the critical intracavity photon number $n_c = \gamma^2/2g_0^2 = 0.04$. Therefore, one is able to perform the transmission spectroscopy measurement with a weak probe laser to obtain the ground-state energy spectrum and atomic population since different quantum phases are, in general, characterized by their specific dispersion relations. The transmission (of this probe laser through the cavity) versus the

detuning may be monitored and/or detected by counting photons out of the cavity. Only when the probe laser frequency matches a system in resonance, the corresponding transmission is anticipated [27].

In summary, we have established an extended Dicke model and designed a feasible experimental setup with the remarkable controllable parameters. An exotic phase diagram has been obtained, which covers various phenomena from quantum optics to the BEC and reveals particularly several novel quantum phase transitions.

We thank S. L. Zhu, D. L. Zhou, L. B. Shao, and Z. Y. Xue for helpful discussions. This work was supported by the RGC of Hong Kong under Grant Nos. HKU7045/05P and HKU74049/07P, the URC fund of HKU, the NSFC under Grant Nos. 10429401, 10775091 and 10704049, and the State Key Program for Basic Research of China (No. 2006CB921800).

* Electronic address: zwang@hkucc.hku.hk

- [1] I. Bloch, *Nature Physics* **1**, 23 (2005)
- [2] C. Maschler, and H. Ritsch, *Phys. Rev. Lett.* **95**, 260401 (2005).
- [3] I. B. Mekhov, C. Maschler, and H. Ritsch, *Nature Physics* **3**, 319 (2007).
- [4] I. B. Mekhov, C. Maschler, and H. Ritsch, *Phys. Rev. Lett.* **98**, 100402 (2007).
- [5] I. B. Mekhov, C. Maschler, and H. Ritsch, *Phys. Rev. A* **76**, 053618 (2007).
- [6] H. Zoubi, and H. Ritsch, *Phys. Rev. A* **76**, 013817 (2007).
- [7] A. Öttl, S. Ritter, M. Köhl, and T. Esslinger, *Phys. Rev. Lett.* **95**, 090404 (2005).
- [8] T. Bourdel *et al.*, *Phys. Rev. A* **73**, 043602 (2006).
- [9] S. Slama, S. Bux, G. Krenz, C. Zimmermann, and P. W. Courteille, *Phys. Rev. Lett.* **98**, 053603 (2007).
- [10] S. Slama, G. Krenz, S. Bux, C. Zimmermann, and P. W. Courteille, *Phys. Rev. A* **75**, 063620 (2007).
- [11] K. W. Murch, K. L. Moore, S. Gupta, and D. M. Stamper-Kurn, arxiv: 0706.1005 (2007).
- [12] S. Gupta, K. L. Moore, K. W. Murch, and D. M. Stamper-Kurn, *Phys. Rev. Lett.* **99**, 213601 (2007).
- [13] Y. Colombe *et al.*, *Nature (London)* **450**, 272 (2007).
- [14] F. Brennecke *et al.*, *Nature (London)* **450**, 268 (2007).
- [15] S. Inouye *et al.*, *Nature (London)* **392**, 151 (1998).
- [16] R. H. Dicke, *Phys. Rev.* **93**, 99 (1954).
- [17] K. Hepp, and E. H. Lieb, *Ann. Phys. (N. Y.)* **76**, 360 (1973).
- [18] Y. K. Wang, and F. T. Hioes, *Phys. Rev. A* **7**, 831(1973).
- [19] C. Emary, and T. Brandes, *Phys. Rev. E* **67**, 066203 (2003).
- [20] Y. Li, Z. D. Wang, and C. P. Sun, *Phys. Rev. A* **74**, 023815 (2006).
- [21] F. Dimer, B. Estienne, A. S. Parkins, and H. J. Carmichael, *Phys. Rev. A* **75**, 013804 (2007).
- [22] G. Chen, Z. D. Chen, and J.-Q. Liang, *Phys. Rev. A* **76**, 045801 (2007).
- [23] M. G. Moore, O. Zobay, and P. Meystre, *Phys. Rev. A* **60**, 1491 (1999).
- [24] D. S. Hall, M. R. Matthews, C. E. Wieman, and E. A. Cornell, *Phys. Rev. Lett.* **81**, 1543 (1998).
- [25] The first-order derivative of the ground-state energy with respect to v is continuous at $v = -u$, but its second-order deriva-

tive has a discontinuity at the same point.

- [26] M. Jääskeläinen, and P. Meystre, Phys. Rev. A **71**, 043603 (2005).
- [27] A. Öttl, S. Ritter, M. Köhl, and T. Esslinger, Rev. Sci. Instrum. **77**, 063118 (2006).